Global and Planetary Change 136 (2016) 82–95

Contents lists available at ScienceDirect

Global and Planetary Change

journal homepage: www.elsevier.com/locate/gloplacha

Hydrological response to future climate changes for the major upstream river basins in the Tibetan Plateau

F. Su [a,b,*], L. Zhang [a,c], T. Ou [d,e], D. Chen [d], T. Yao [a,b], K. Tong [a], Y. Qi [f]

[a] Key Laboratory of Tibetan Environment Changes and Land Surface Processes, Institute of Tibetan Plateau Research, Chinese Academy of Sciences, Beijing, 100101, China
[b] CAS Center for Excellence in Tibetan Plateau Earth Sciences, Beijing, 100101, China
[c] Power China Huadong Engineering Corporation Limited, Hangzhou, 310014, China
[d] Department of Earth Sciences, University of Gothenburg, Gothenburg, Sweden
[e] Faculty of Earth Systems & Environmental Sciences, Chonnam National University, Gwangju, South Korea
[f] School of Public Policy and Management, Tsinghua University, Beijing, 100084, China

ARTICLE INFO

Article history:
Received 8 January 2015
Received in revised form 3 June 2015
Accepted 22 October 2015
Available online 23 October 2015

Keywords:
Tibetan Plateau
Future climate change
River runoff
Glacier melt
Hydrological response

ABSTRACT

The impacts of future climate change on water balance for the headwater basins of six major rivers in the Tibetan Plateau are assessed using the well-established VIC-glacier land surface hydrological model driven by composite projections of 20 CMIP5 GCMs under scenarios RCP2.6, RCP4.5, and RCP8.5. At the plateau scale, the annual precipitation is projected to increase by 5.0–10.0% in the near term (2011–2040) and 10.0–20.0% in the long term (2041–2070) relative to the reference period 1971–2000. The annual temperature is projected to increase for all the scenarios with the greatest warming in the northwest (2.0–4.0 °C) and least in the southeast (1.2–2.8 °C). The total runoff of the study basins would either remain stable or moderately increase in the near term, and increase by 2.7–22.4% in the long term relative to the reference period, as a result of increased rainfall-induced runoff for the upstream of the Yellow, Yangtze, Salween, and Mekong and increased glacier melt for the upper Indus. In the upper Brahmaputra, more than 50.0% of the total runoff increase is attributed to the increased glacier melt in the long run. The annual hydrograph remains practically unchanged for all the monsoon-dominated basins. However, for the westerly-controlled basin (upper Indus), an apparent earlier melt and a relatively large increase in spring runoff are observed for all the scenarios, which would increase water availability in the Indus Basin irrigation scheme during the spring growing season.

1. Introduction

Major Asian rivers originate from the Tibetan Plateau (TP) and adjacent mountains (Fig. 1), which contains the largest number of glaciers outside the polar regions (Yao et al., 2008). Studies based on meteorological observations, reanalysis data and ice core records have suggested a warming trend (0.16 °C/decade to 0.36 °C/decade) over the TP in recent decades (Thompson et al., 2000; Yao et al., 2000; Liu and Chen, 2000; Frauenfeld et al., 2005; Wu et al., 2007; Xu et al., 2008; Wang et al., 2008). Global climate models from the fifth phase of the Coupled Model Intercomparison Project (CMIP5) also project a warming trend of 0.47 °C/10a to 0.73 °C/10a over the TP in the 21st century under emission scenario RCP8.5 (Su et al., 2013). Along with the warming climate, several studies have reported that the TP glaciers are largely experiencing shrinkage especially in the monsoon-dominated parts of Himalayas (Yao et al., 2004, 2007, 2012; Bolch et al., 2012). The implications of the warming climate and glacier melt in the TP have resulted in a major concern for the water resources downstream (Immerzeel et al., 2010; Kaser et al., 2010).

It was suggested that vanishing glaciers would reduce water supply in the glaciated regions of the TP and adjacent mountains (Barnett et al., 2005). However, the relative importance of meltwater to runoff of major rivers differs fundamentally under different precipitation regimes in the TP (Bookhagen and Burbank, 2010; Immerzeel et al., 2010; Zhang et al., 2013; Bliss et al., 2014). Runoff is influenced not only by glacier- and snow-melt, but also by precipitation. The climate in the TP is mostly dominated by the monsoon systems in the southeast and the westerlies in the northwest. Annual precipitation exhibits an east to west gradient, ranging from over 1500 mm per year in the southeast to less than 100 mm per year in the west (Tong et al., 2014). In the summer months, the southeast monsoon produces heavy precipitation, whereas in the western part, westerly winds cause winter precipitation (Rees and Collins, 2006; Bookhagen and Burbank, 2010). This spatial variability of precipitation influences meltwater regimes, which in turn affect the availability of water for the rivers downstream. Thus, the hydrological response to climate change will be different due to the differences in the source of runoff, climatic conditions and physiological characteristics of the basins.

* Corresponding author at: Institute of Tibetan Plateau Research, CAS, Beijing, 100101, China.
E-mail address: fgsu@itpcas.ac.cn (F. Su).

http://dx.doi.org/10.1016/j.gloplacha.2015.10.012
0921-8181/

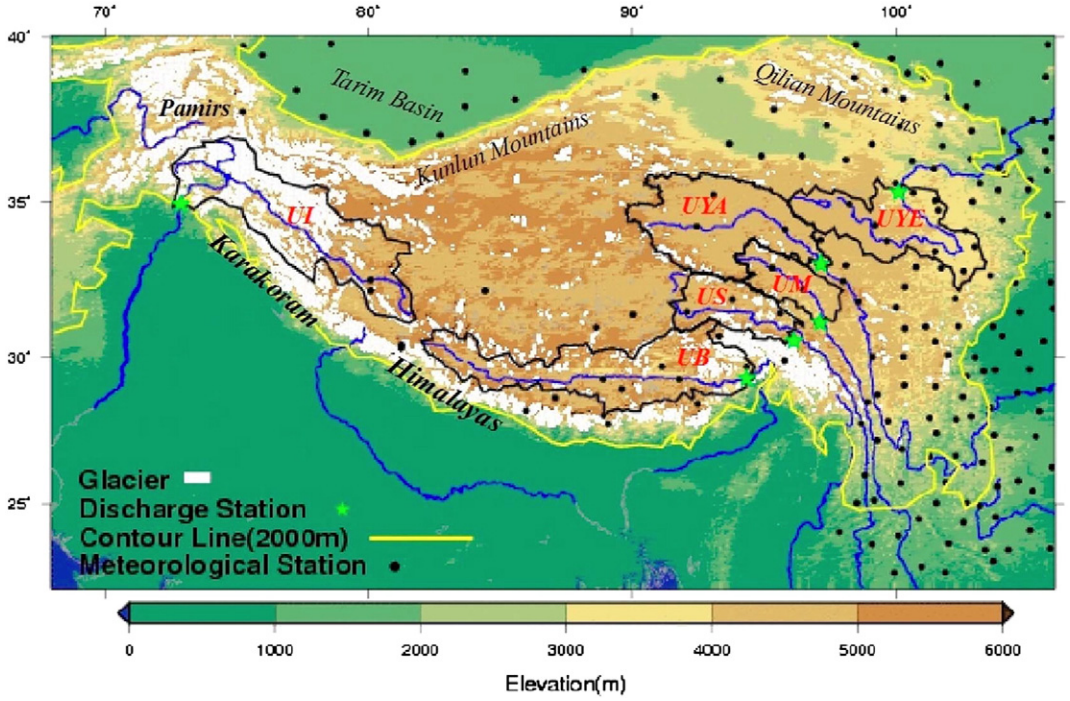

Fig. 1. Topography, rivers (blue lines), boundaries of investigated six basins (black lines) and location of the 176 meteorological stations used for the climate forcing for the period 1971–2000. The UYE, UYA, UM, US, UB and UI represent the upstream of the Yellow, Yangtze, Mekong, Salween, Brahmaputra, and Indus rivers, respectively.

Quantifying the potential impacts of future climate changes on glaciers and river flow over the TP is essential to assist policy-makers and water managers in adopting strategies depending on the state of scientific understanding. A hydrological model driven by hypothetical climatic conditions or climate model projections has been a commonly used approach for assessing the hydrologic consequences of climatic changes. However, most of the existing hydrological impact studies over the TP have focused on branches of the Indus River system (mostly affected by the westerlies) and small Himalayan rivers (Singh and Bengtsson, 2005; Rees and Collins, 2006; Tahir et al., 2011; Jeelani et al., 2012; Immerzeel et al., 2009, 2012, 2013). Less attention has so far been given to a comprehensive understanding of plateau-scale effects. Moreover, uncertainties in climate change scenarios and/or hydrological models have produced large discrepancies among the few available twenty-first century projections of water availability from the TP rivers (e.g., Immerzeel et al., 2010; Lutz et al., 2014). Singh and Bengtsson (2005) investigated the impact of warmer climate on melt and evaporation of a branch of the Indus River system using a conceptual snowmelt model. The results suggest a reduction of 18% of melt water from snowfed basins and an increase of 33% from glacierfed basins under an assumed temperature scenario ($t + 2$ °C). Rees and Collins (2006) investigated the regional differences in response of flow in glacier-fed Himalayan rivers with a temperature-index-based hydro-glaciological model under a uniform warming scenario (0.06 °C year^{-1}) and suggested that the melt water component in the total runoff would rapidly decrease from west to east. Immerzeel et al. (2009) assessed the effects of climate change on streamflow of upper Indus using the Snowmelt Runoff Model (SRM) with a regional climate model's projections under assumed glacier extent scenarios. The total runoff of the upper Indus was projected to increase 7% by the end of 21st century relative to 2001–2005 under a 50% decrease of glacier extent scenario. Using the same SRM model, Immerzeel et al. (2010) provided an assessment of future water availability from five river basins (Indus, Brahmaputra, Ganges, Yellow, and Yangtze rivers) in the TP under different climate and glacier area scenarios. Their results suggest that all the basins except the Yellow would have a decrease in mean annual flow over the period 2046–2065 relative to 2000–2007. A more recent study (Lutz et al., 2014) using a distributed cryospheric-hydrological model and an ensemble of the latest GCM outputs, however, projects an increase in runoff at least until 2050, due to primarily an increase in precipitation in the upper Ganges, Brahmaputra, Salween and Mekong basins and accelerated melt in the upper Indus Basin. The

Table 1
Characteristics of the six source river basins in the Tibetan Plateau. Glacier areas are based on a dataset from the "Environmental & Ecological Science Data Center for West China" (http://westdc.westgis.ac.cn/data/ff75d30a-ee7d-4610-a5a3-53c73964a237) and the Randolph Glacier Inventory (http://www.glims.org/RGI/).

Basins		Yellow	Yangtze	Mekong	Salween	Brahmaputra	Indus
Control stations		Tangnaihai	Zhimenda	Changdu	Jiayuqiao	Nuxia	Besham
Location	Latitude (°N)	35.30	33.02	31.11	30.51	29.27	34.92
	Longitude (°E)	100.09	97.13	97.11	96.12	94.34	72.88
Drainage area (km^2)		121,972	137,704	53,800	69,384	191,235	164,867
Percent of total basin area (%)		16.22	7.61	6.77	20.91	30.89	13.91
Glacier area (km^2)		134.16	1308.19	225.96	1151.58	4225.20	15,325.20
Percent of drainage area (%)		0.11	0.95	0.42	1.70	2.10	9.46

Table 2
Twenty GCMs used for perturbing the historical forcing data.

Modeling group	Institute ID	Model name	Atmosphere resolution (longitude × latitude in degrees)
Beijing Climate Center, China Meteorological Administration	BCC	BCC-CSM1.1	2.8125 × 2.7906
College of Global Change and Earth System Science, Beijing Normal University	GCESS	BNU-ESM	2.8125 × 2.7906
Canadian Centre for Climate Modeling and Analysis	CCCMA	CanESM2	2.8125 × 2.7906
National Center for Atmospheric Research	NCAR	CCSM4	1.2500 × 0.9424
The First Institute of Oceanography, SOA, China	FIO	FIO-ESM	2.8125 × 2.7906
NOAA Geophysical Fluid Dynamics Laboratory	NOAA GFDL	GFDL-CM3	2.5000 × 2.0000
		GFDL-ESM2G	2.5000 × 2.0225
		GFDL-ESM2M	2.5000 × 2.0225
NASA Goddard Institute for Space Studies	NASA GISS	GISS-E2-R	2.5000 × 2.0000
National Institute of Meteorological Research/Korea Meteorological Administration	NIMR/KMA	HadGEM2-AO	1.8750 × 1.2500
Met Office Hadley Centre	MOHC	HadGEM2-ES	1.8750 × 1.2500
Institut Pierre-Simon Laplace	IPSL	IPSL-CM5A-LR	3.7500 × 1.8947
		IPSL-CM5A-MR	2.5000 × 1.2676
Japan Agency for Marine-Earth Science and Technology, Atmosphere and Ocean Research Institute (The University of Tokyo), and National Institute for Environmental Studies	MIROC	MIROC-ESM	2.8125 × 2.7906
		MIROC-ESM-CHEM	2.8125 × 2.7906
Atmosphere and Ocean Research Institute (The University of Tokyo), National Institute for Environmental Studies, and Japan Agency for Marine-Earth Science and Technology	MIROC	MIROC5	1.4063 × 1.4008
Max Planck Institute for Meteorology	MPI-M	MPI-ESM-LR	1.8750 × 1.8653
Meteorological Research Institute	MRI	MRI-CGCM3	1.1250 × 1.1215
Norwegian Climate Centre	NCC	NorESM1-M	2.5000 × 1.8947
		NorESM1-ME	2.5000 × 1.8947

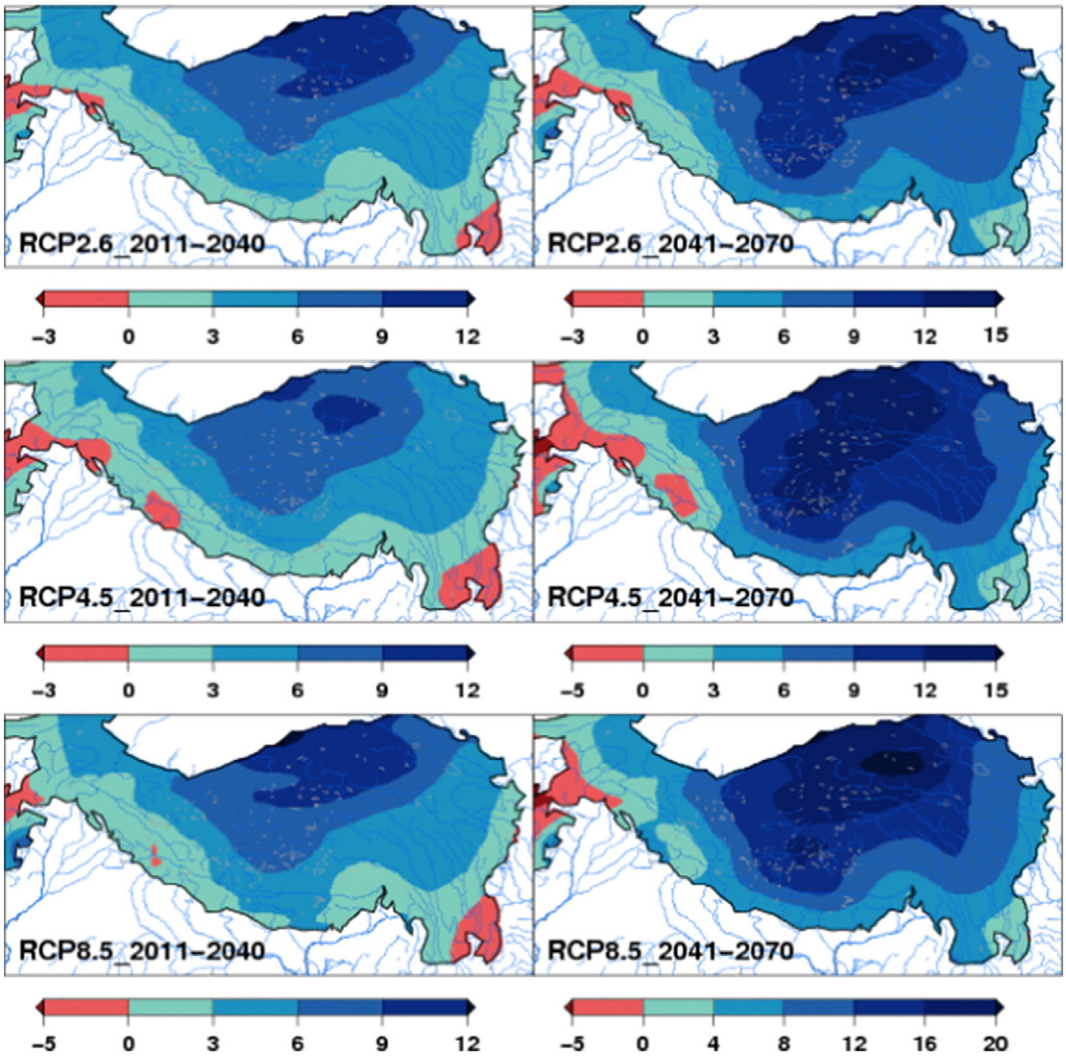

Fig. 2. Composite change factors (%) of mean annual precipitation for the periods 2011–2040 and 2041–2070 with respect to the baseline 1971–2000 under scenarios RCP2.6, RCP4.5, and RCP8.5.

existing studies suggest that the projected river runoff in the TP is largely dependent on the hydrological model and the projected climatic scenarios used in the assessment. This makes it difficult to draw consistent conclusions on the impact of climate change on water resources. Here we use a distributed, process-based land surface hydrological model, whose physical basis allows better understanding of the land surface-vegetation system and a more realistic representation of relevant processes.

Zhang et al. (2013) provided a broad picture for the hydrologic regimes of the major upstream river basins in the TP, including the source regions of the Yellow (UYE), Yangtze (UYA), Mekong (UM), Salween (US), Brahmaputra (UB) and Indus (UI) rivers (Fig. 1), based on long-term hydrological and meteorological observations. In their work, a hydrologic modeling framework was established over the entire TP at 1/12 × 1/12° grids (about 10 km × 10 km) with the variable infiltration capacity (VIC) land surface hydrology model linked with a degree-day glacier scheme (VIC-glacier model), and the contributions to total runoff from rainfall, snowmelt and glacier melt for the selected source river basins were quantified based on the VIC-glacier model historical simulations. In the present study, we extend the work of Zhang et al. (2013), with an aim to investigate the potential impacts of future climate changes on the hydrology of the six source river basins (UYE, UYA, UM, US, UB and UI, Table 1) in the TP. More specific goals are to: 1) develop a framework for systematic assessment of hydrological consequences for the major upstream basins in the TP using a well-established land surface hydrological model; and 2) use the framework to quantify the contribution of rainfall, snowmelt, and glacier runoff to the total runoff for the river basins under a number of future climate change scenarios.

2. Study basins, model, and data

2.1. Study basins

Our study area is limited to the domain with the elevation above 2000 m, focusing on the six source river basins (UYE, UYA, UM, US, UB and UI) in the plateau (Fig. 1). The six basins occupy about 744,000 km^2 and cover 30.0% of the total TP area above 2000 m a.s.l. Four basins (UYE, UYA, UM, and US) are located in the monsoon-dominated southeast of the TP; the western basin of UI is largely affected by the westerlies with large precipitation occurring in the winter and spring, often in the form of snow; while the UB in the south is affected by both monsoon and westerly systems. Among the six basins, the UI has the largest glacier coverage (about 15,325 km^2, close to 9.5% of the basin area), and the UYE has the smallest glacier area (about 134 km^2 and 0.1% of the UYE basin; Table 1). The UB has the second largest glacier area (4225 km^2), covering

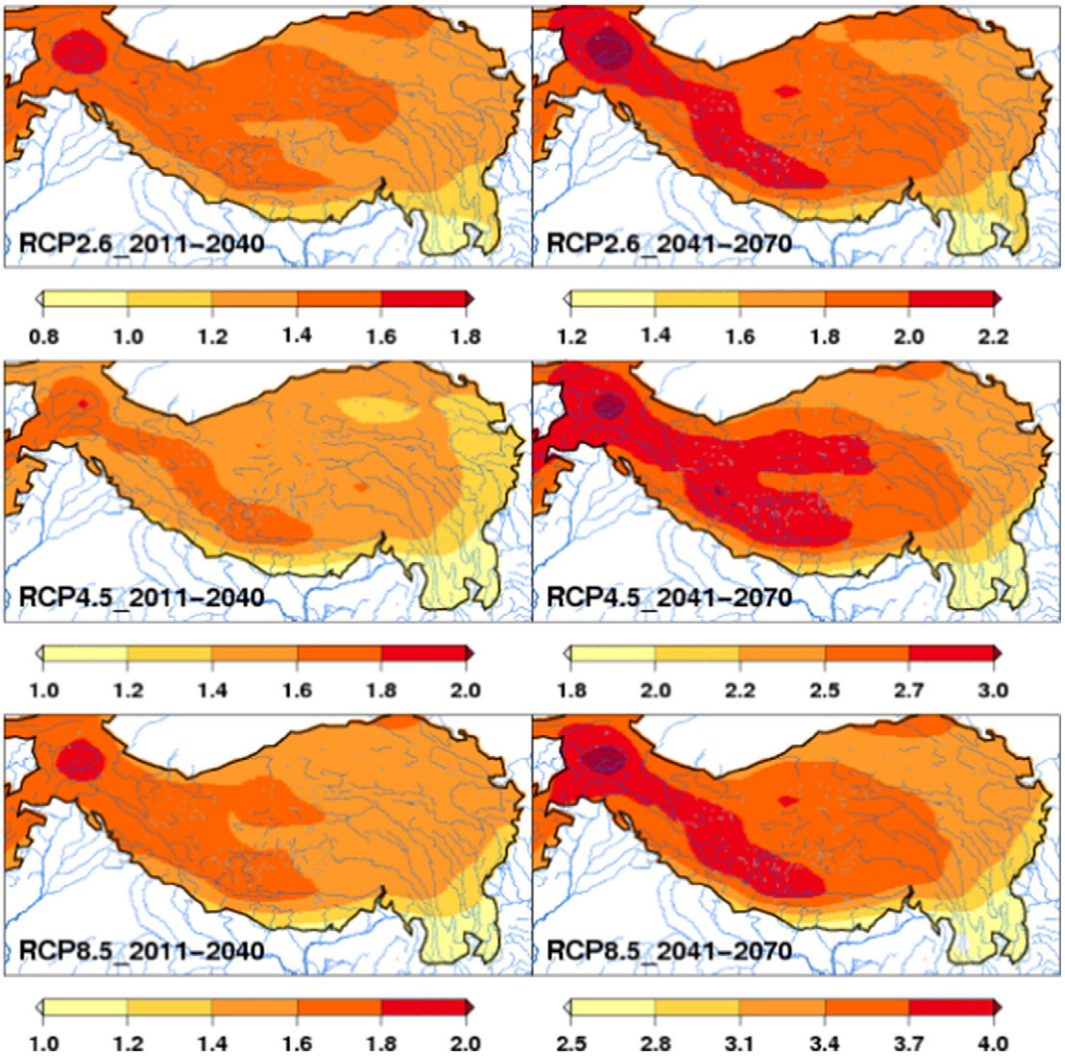

Fig. 3. Composite change factors (°C) of mean annual temperature for the periods 2011–2040 and 2041–2070 with respect to the baseline 1971–2000 under scenarios RCP2.6, RCP4.5, and RCP8.5.

about 2.1% of the basin, while the UYA, UM, and US have less glacier coverage (about 1.0%, 0.4%, and 1.7% of the basin area, respectively). Previous model simulations (Zhang et al., 2013) suggest that the importance of glacier-melt water is minor for the UYE and UM (less than 2.0% of the annual runoff), and moderate for the UYA and US (5.0–7.0%). Glacier water becomes more important for the UB (about 12.0% of the annual runoff), and extremely important for the UI, contributing to about 48.0% of the annual runoff.

2.2. The VIC-glacier model

VIC is a grid-based land surface scheme which parameterizes the dominant hydrometeorological processes taking place at the land surface-atmosphere interface (Liang et al., 1994, 1996). The model solves both surface water and energy balances over a grid mesh. Surface runoff and baseflow for each cell are routed to the basin outlet through a channel network (Lohmann et al., 1998). The critical elements in the model that are particularly relevant to cold land implementations include: (1) a two layer snow model based on energy balance (Cherkauer and Lettenmaier, 1999; Storck and Lettenmaier, 1999) which represents snow accumulation and ablation in a ground pack and an overlying forest canopy, where present; and (2) a frozen soil/permafrost algorithm (Cherkauer and Lettenmaier, 1999, 2003) that solves for soil ice contents within each vegetation type and represents the effects of frozen soils on the surface energy balance and runoff generation. The VIC model has been widely used to assess the impact of climate change on U.S. hydrology (Hamlet and Lettenmaier, 1999; Payne et al., 2004; Christensen et al., 2004; Vicuna et al., 2007; Maurer, 2007; Christensen and Lettenmaier, 2007; Hayhoe et al., 2007; Elsner et al., 2010), the Nile River basin in Africa (Beyene et al., 2010), and on the snow hydrology of global river basins (Barnett et al., 2005; Adam et al., 2009). However, the glacier-melt water was not considered in the previous applications. Here, we use the VIC land surface model linked with a simple degree-day glacier algorithm (Hock, 2003), which was referred to as VIC-glacier model in Zhang et al. (2013).

The initial glacier distribution dataset was from the "Environmental & Ecological Science Data Center for West China" (http://westdc.westgis.ac.cn/data/ff75d30a-ee7d-4610-a5a3-53c73964a237) and the Randolph Glacier Inventory (Arendt et al., 2012) which is complete for UI and includes recent data (http://www.glims.org/RGI/). These data are used for calculating the initial glacier fraction within each gird cell.

The total runoff from each grid cell is calculated as the follows:

$$R(i) = f \times G_i + (1-f) \times R_{\text{vic}} \quad (1)$$

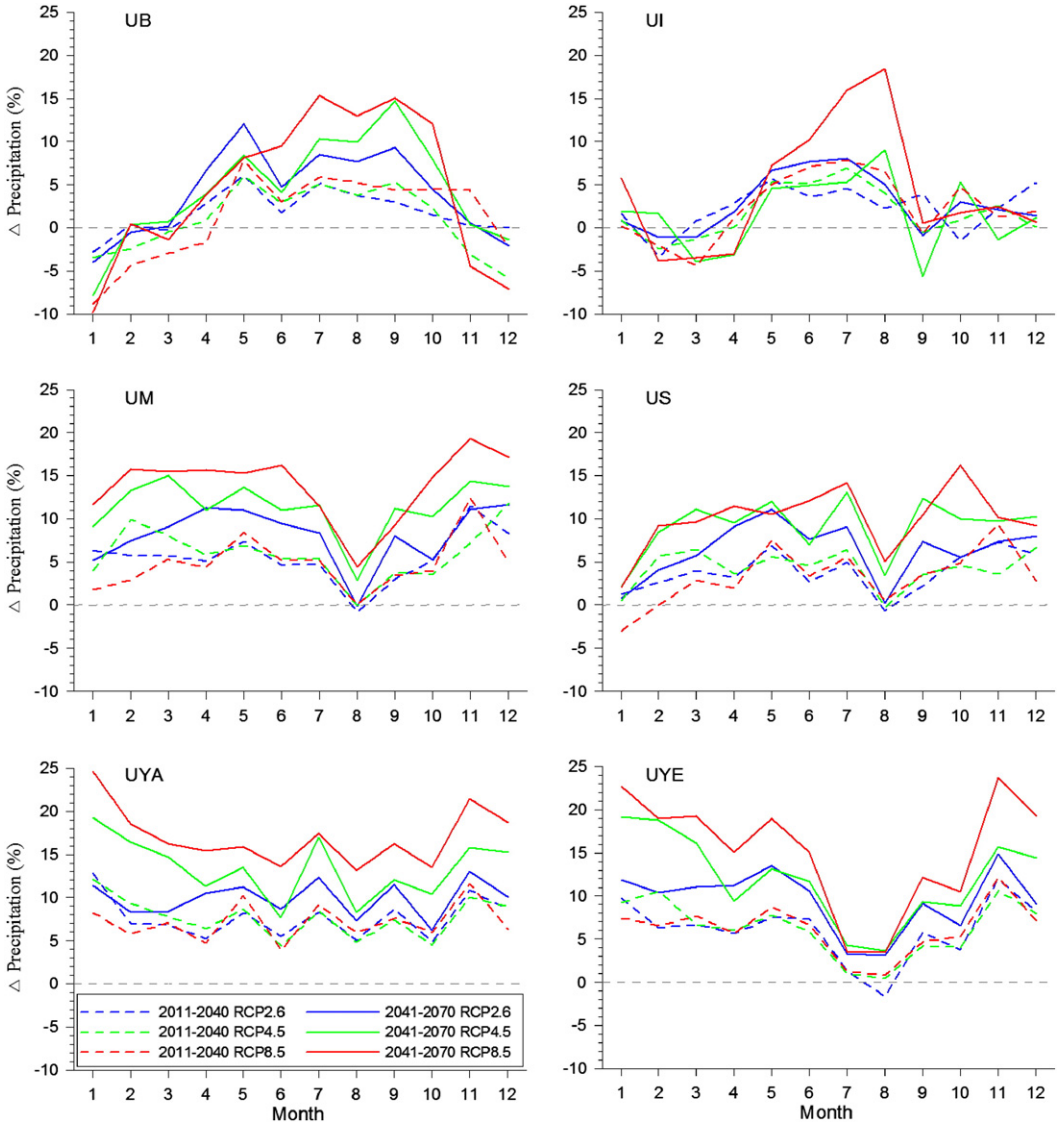

Fig. 4. Seasonal cycle of averaged precipitation (P_{frac}) changes over the six selected source river basins for the periods 2011–2040 and 2041–2070 with respect to the baseline 1971–2000 under scenarios RCP2.6, RCP4.5, and RCP8.5.

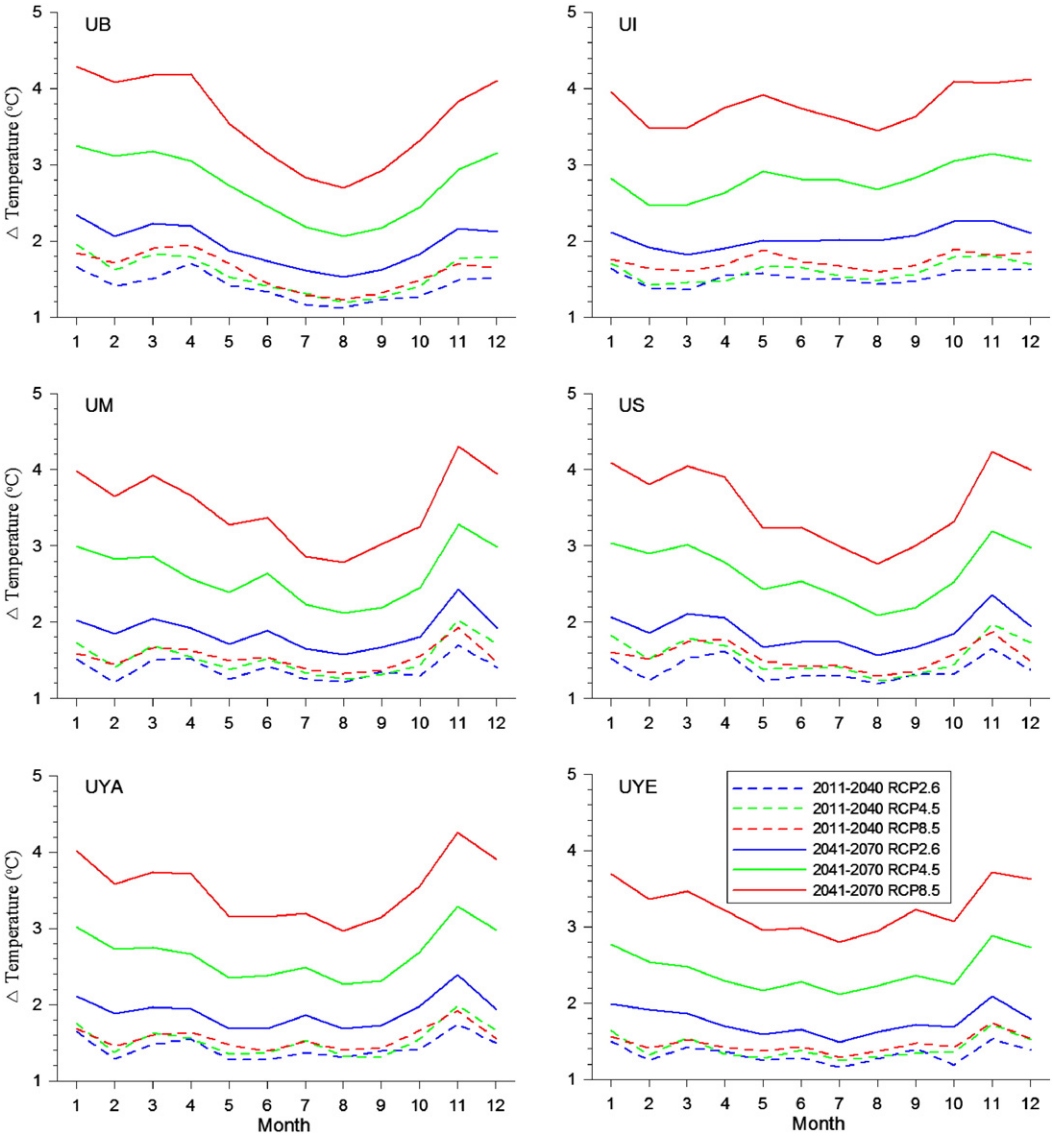

Fig. 5. Same as Fig. 4, but for ΔT (°C).

where $R(i)$ is total runoff (mm) in a grid i; f is glacier area fraction within the grid cell; R_{vic} is runoff (mm) from ice-free area calculated by the VIC model; and G_i is glacier runoff (mm) from glaciated area, including liquid precipitation, and snow/glacier melt water (M_i, mm). The meltwater M_i from the glaciated area in grid i is calculated as:

$$M_i = \begin{cases} \text{DDF} \times T_i; & T_i > 0 \\ 0; & T_i \le 0 \end{cases} \quad (2)$$

where DDF is the degree-day factor for glacier or snowmelt (mm °C^{-1} day^{-1}). T_i (°C) is daily mean air temperature above glacier surface. When there is a snowpack on the glacier, the snow melts first before the glacier starts melt. The temperature over the glacier area within each grid cell is adjusted by a commonly used temperature lapse rate (0.65 °C/100 m).

We use the volume–area scaling relation (Bahr et al., 1997; Radić et al., 2007, 2008; Radić and Hock, 2010; Liu et al., 2003) to derive glacier volume at the regional scales. At $t = 0$ the initial ice volume for each basin was determined using initial glacier area from the glacier distribution dataset. This initial volume was updated every 10 years with the accumulation of snowfall and melt water (mass balance) for all the glaciated cells. The updated glacier area at $t = 1$ was determined by inverting the volume–area scaling relation with the updated volume. This procedure was repeated for all the VIC-glacier simulation periods.

The parameters most often adjusted during calibration of the VIC model include the infiltration parameter (b_inf), the depth of the first and second soil layers (d1, d2), and three base flow parameters (Ds, Ws, Ds_{max}) (Nijssen et al., 2001; Su et al., 2005). The parameter b_inf, with a typical range of 0–0.4, defines the shape of the variable infiltration capacity curve; an increase of b_inf tends to enhance runoff production, while a decrease of b_inf tends to reduce runoff. The maximum moisture storage capacity is dynamically determined by the change in soil thickness. Thicker soil depths have higher moisture storage capacity, thus less runoff production. Three base flow parameters determine how quickly the water storage in the third layer evacuates and are generally less sensitive than parameters b_inf and d2. The topsoil layer depth (d1) for each grid cell was set to 5–10 cm as suggested in Liang et al. (1996). Therefore, only the infiltration parameter (b_inf) and the second soil depth (d2) were targeted for intensive calibration (Zhang et al., 2013).

In Zhang et al. (2013), snow factor is 4.1 mm °C^{-1} day^{-1} for most basins, and the ice factors are 4.7 mm °C^{-1} day^{-1} for UYE,

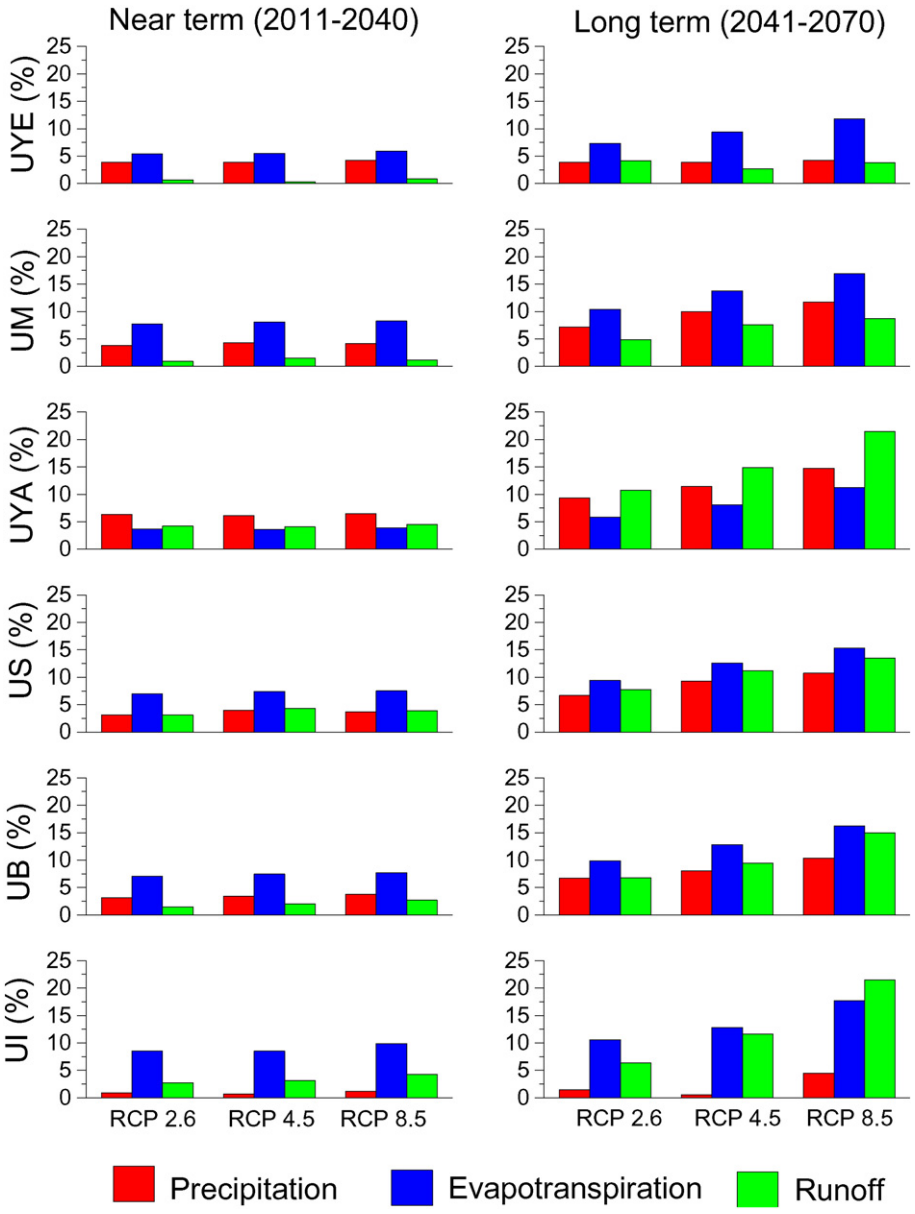

Fig. 6. Projected changes in mean annual precipitation, evapotranspiration, and total runoff for 2011–2040 and 2041–2070 relative to the baseline period 1971–2000 under the scenarios considered over the headwater basin of the six rivers.

7.1 mm $°C^{-1}$ day^{-1} for UYA and US, 13.8 mm$°C^{-1}$ day^{-1} for UM, and 9.0 $°C^{-1}$ day^{-1} mm for UB. For the UI, the snow factor is set at 4.0 mm $°C^{-1}$ day^{-1}, and ice factor is 7.0 mm $°C^{-1}$ day^{-1}. The VIC-glacier model has been calibrated and validated with about 30–40 years of observed precipitation and streamflow data over the basins, and the annual bias is generally within ±5%. In this work, the model set-up at the 1/12° × 1/12° grids, including VIC vegetation and soil parameters and degree-day factors for snow and ice are all adopted from Zhang et al. (2013). No further model calibrations are performed for the baseline simulations of 1971–2000.

2.3. Historical forcing data

We chose 1971–2000 as the baseline period. The meteorological forcing data for the VIC model include daily precipitation (P), maximum temperature (T_{max}), minimum temperature (T_{min}), and wind speed. The vapor pressure, incoming shortwave radiation and net long-wave radiation were calculated using algorithms described in Maurer et al. (2002). The daily P, T_{max}, T_{min}, and wind speed from 176 stations over the TP and adjacent regions (Fig. 1) during 1971–2000 were collected from the China Meteorological Administration (CMA). All the station data were gridded to the 1/12 × 1/12° resolution using the inverse distance weighting method. Because the 176 stations are limited within China (Fig. 1) and the precipitation station data for the UI is not available, a gauge-based precipitation product APHRODITE (Asian Precipitation — Highly Resolved Observational Data Integration Towards Evaluation of Water Resources) project (http://www.chikyu.ac.jp/precip/) (Yatagai et al., 2009) was used in the historical model runs (1971–2000) for the river basin UI. The APHRODITE is a daily gridded precipitation dataset at 1/4° resolution, which has been created by collecting rain gauge observation data (1961 onward). In this analysis, the 1/4° APHRODITE precipitation data were regridded to the 1/12° grids by the nearest neighbor approach. For the historic (1971–2000) simulation, the VIC-glacier model was forced with daily gridded precipitation, maximum and minimum temperature, and wind speed over the six source river basins (Fig. 1).

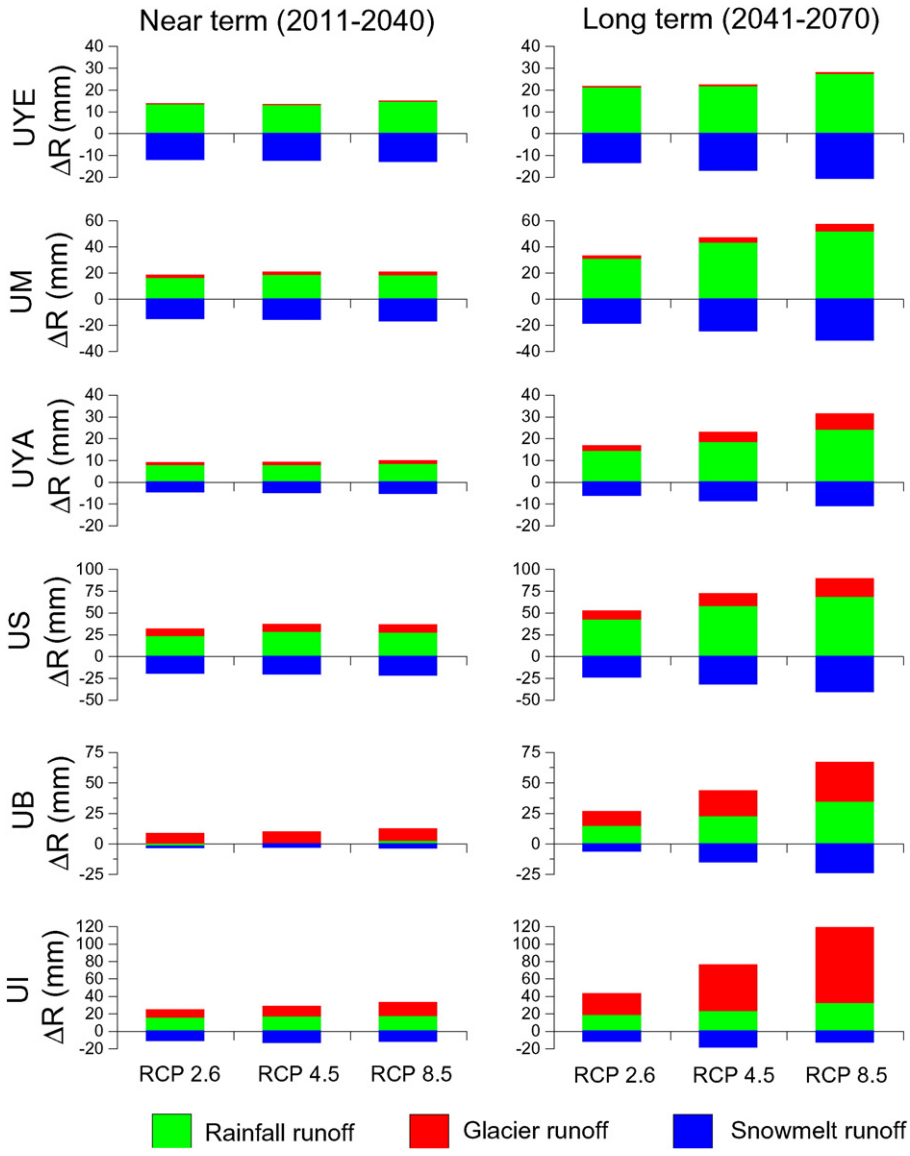

Fig. 7. Changes in mean annual rainfall runoff, snowmelt runoff, and glacier runoff for 2011–2040 and 2041–2070 relative to the baseline period 1971–2000 under the scenarios considered over the six source river basins.

2.4. Future forcing data

Outputs of monthly precipitation and temperature from 20 GCMs (Table 2) in the CMIP5 (Taylor et al., 2012) are used to generate the future forcing data for the hydrology model. Scenarios RCP2.6, RCP4.5, and RCP8.5 are selected for investigating the 21st century climate projections over the TP (Van Vuuren et al., 2011; Moss et al., 2010). RCP8.5 is the highest emission scenario used by IPCC AR5, with an increasing radiative forcing to 8.5 W/m^2 at 2100; RCP2.6, by contrast, represents the lowest emission scenario throughout the 21st century, with a forcing peaking in 2035 at around 3 W/m^2 and decreasing to 2.6 W/m^2 by 2100; and RCP4.5 represents a medium-low emission scenario, with a stabilization of radiative forcing at 4.5 W/m^2 in 2100 (Cubasch et al., 2013). One of the CMIP5's aims is to provide projections of future climate on two time scales, near term (out to about 2035) and long term (out to 2100 and beyond). Therefore, we focus on the CMIP5 model projections over the TP at two time scales: 2011–2040 (near term) and 2041–2070 (long term).

The delta method (Gleick, 1986; Hay et al., 2000) is used to develop climate change scenarios considered. The method builds on the principles that the climate change simulated by a GCM (typically a difference for temperature and a percentage change for precipitation) can effectively avoid a large part of the model bias. All the monthly fields of GCM temperature and precipitation are regridded to the 1/12° × 1/12° grids via linear interpolation. Evaluation of 24 CMIP5 models over the TP (Su et al., 2013) suggest that: 1) multi-model ensemble mean shows better agreement with observations than does any single model; 2) over the next 90 years, projections differ much more among models than among emissions scenarios for both temperature and precipitation. Therefore, we have more confidence in the model ensembles in simulating the TP climate. Similar to the approach used in Adam et al. (2009); Elsner et al. (2010), and Cuo et al. (2011), here, the monthly change factors for each scenario are calculated by comparing the monthly means of the 20 GCM outputs for the 30-year future time slices (2011–2040 and 2041–2070) to the monthly GCM-average historic run output for the 30-year baseline period (1971–2000). For each calendar month and each 1/12° grid cell, the precipitation change factor for the time

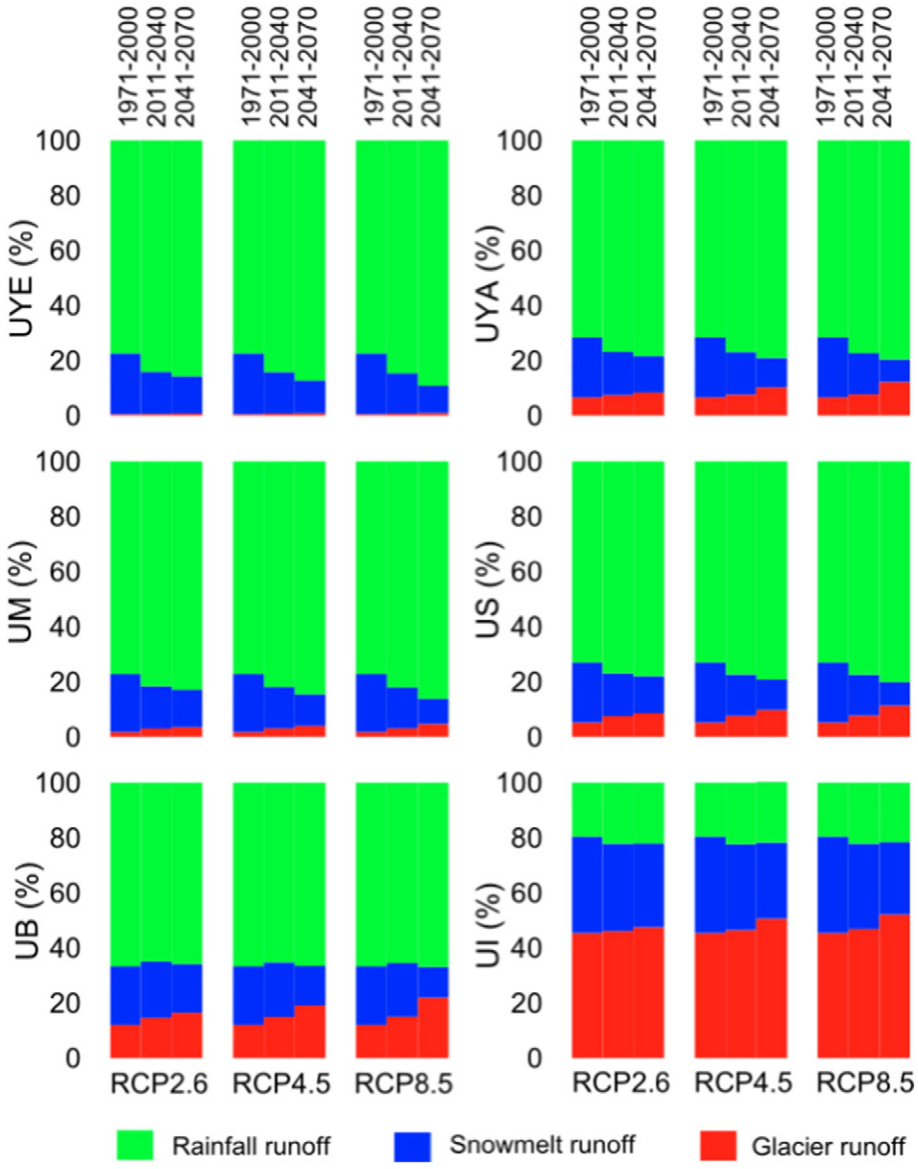

Fig. 8. Contribution of rainfall, snowmelt, and glacier runoff to the total runoff in different periods under the scenarios considered over the headwater basin of the six rivers.

slice 2011–2040 is calculated by:

$$P_{\text{frac}} = P_{\text{GCM}(2011-2040)} \div P_{\text{GCM}(1971-2000)} \quad (4)$$

For cases in which the monthly historical GCM precipitation is zero, P_{frac} is set to one. For temperature, the additive temperature change factor, ΔT, for the 2011–2040 time-slice is calculated by:

$$\Delta T = T_{\text{GCM}(2011-2040)} - T_{\text{GCM}(1971-2000)} \quad (5)$$

The precipitation and temperature change factors for the time-slice 2041–2070 are obtained similarly using Eqs. (4) and (5). The spatially-distributed monthly composite change factors are finally used to perturb the gridded daily observation-based forcing data over the baseline period 1971–2000 and the future simulations are then compared with the baseline simulation using historical climate as the forcing.

3. Projected changes of precipitation and temperature

Figs. 2 and 3 show the average change factors of precipitation (P_{frac}) and temperature (ΔT), respectively, over the entire TP for the periods 2011–2040 and 2041–2070 with respect to the baseline 1971–2000 under scenarios RCP2.6, RCP4.5, and RCP8.5. At the plateau scale, annual precipitation is generally projected to increase by 5.0–10.0% in the near term and 10.0–20.0% in the long term with an increasing south–north gradient, although a slight decrease (<5.0%) is projected for the southwest and southeast corner of the TP. Annual temperature is projected to increase for all scenarios with the greatest warming in the northwest (2.0–4.0 °C) and least in the southeast (1.2–2.8 °C), with the larger warming occurring in the long term.

Runoff is a spatially integrated response of hydrologic processes to climate input. Thus it is necessary to understand the projected climate changes at the basin scale. Figs. 4 and 5 show seasonal cycles of the basin-averaged precipitation (P_{frac}) and temperature (ΔT) changes, respectively. Projected precipitation changes greatly among seasons and basins (Fig. 4). For instance, in the UB, precipitation is mostly projected to increase for the monsoon months (May–Oct) and decrease in the winter months (Dec–Mar) up to 10.0–15.0% for RCP8.5 in the long term. The UI sees a moderate decrease (<5.0%) mostly during Feb–Apr, and an increase during May–Aug (mostly less than 10% except for RCP8.5 in the long term). The basins UM and UYE show similar seasonal changes of precipitation with large increases (5.0–25.0%)

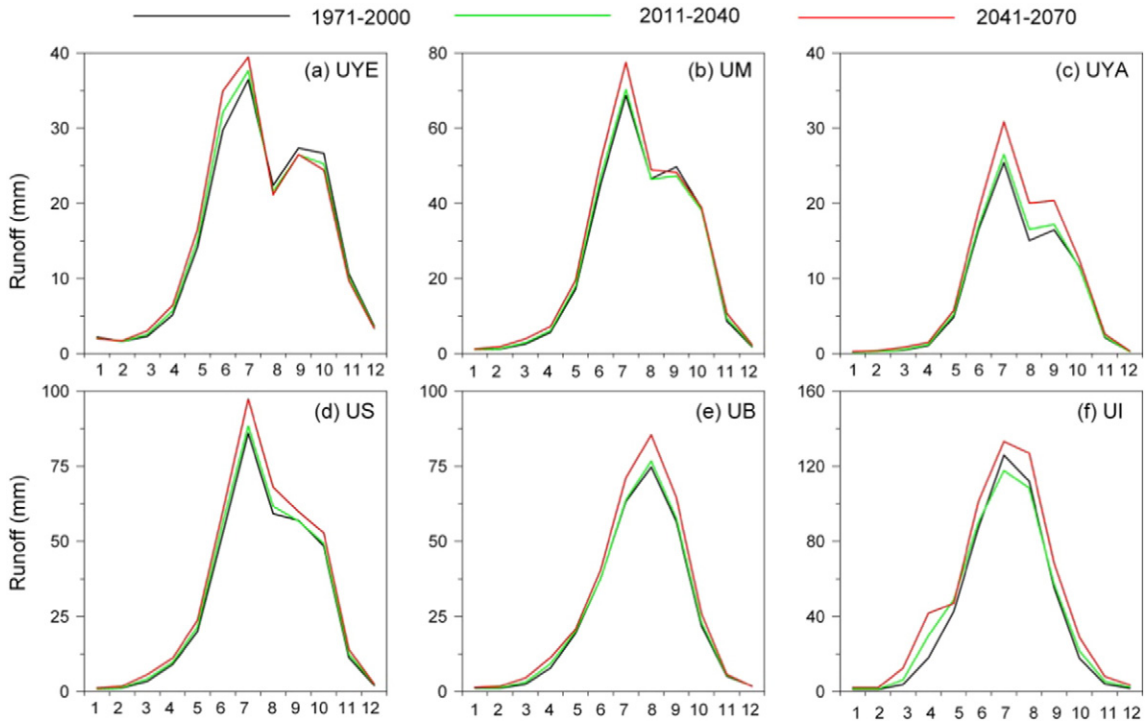

Fig. 9. Seasonal cycle of simulated runoff for the periods 1971–2000, 2011–2040, and 2040–2071 for the six source river basins under scenario RCP8.5.

in all the months except for August (<5.0%), while no apparent seasonality of precipitation changes is observed in the UYA. At the annual basis, the basins UYE, UYA, UM, US, and UB exhibit moderate increase (3.0–7.0%) in mean annual precipitation in the near term and more (6.0–15.0%) in the long term for all scenarios, while the western basin UI shows only slight changes in precipitation (less than 2.0%) until in the long-term period for scenario RCP8.5 (about 4.5% increase).

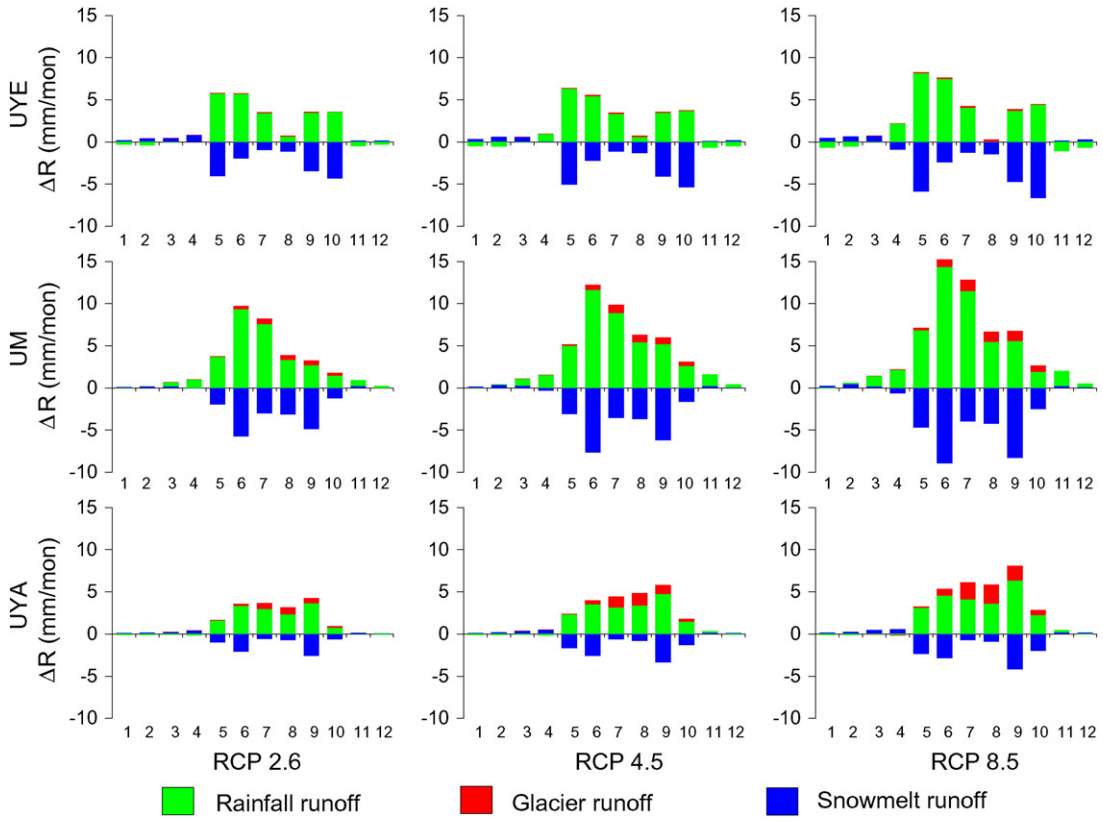

Fig. 10. Seasonal changes in rainfall runoff, snowmelt runoff, and glacier runoff during 2041–2070 relative to the baseline period 1971–2000 for the basins UYE, UM, and UYA, under the scenarios considered.

Temperature is projected to increase for all seasons but with largest warming appearing in winter and spring for all the basins (Fig. 5). The warming rates are mostly less than 2.0 °C in the near term; the greater warming and larger discrepancy (2.0–4.5 °C) among the scenarios are observed in the long term. Mean annual temperature is projected to increase by 1.3–1.7 °C in the near term and 1.7–3.8 °C in the long term. The results of Figs. 4 and 5 suggest that more precipitation and more warming generally appear in the long term than in the near term.

4. Hydrological responses to projected climate changes

4.1. Mean annual changes

Fig. 6 shows projected changes in mean annual precipitation, evapotranspiration, and total runoff. In the near term, the total runoff of the UYE is relatively stable and the other basins exhibit a moderate increase (<5.0%), because the limited increase of precipitation is to large extent compensated by an increase of evapotranspiration (4.0–10.0%) (Fig. 6). In the long term, the total runoff is projected to increase by 10.7–21.4% for the UYA, 4.8–8.7% for the UM and 7.7–13.5% for the US. For the UB and UI, the total runoff in the long term is projected to increase by 6.7–14.4% and 6.3–22.4%, respectively. Along with the larger warming in the long term (Fig. 5), the evapotranspiration is projected to increase by 6.0–18.0%. Although a consistent increase in total runoff is projected for all the basins in the long term, the major cause for the increase is different for different basins.

According to the source of runoff generation, the total runoff is partitioned into three components: rainfall runoff, snowmelt runoff, and glacier runoff. Fig. 7 shows the mean annual changes of each component. For the monsoon-dominated basins, rainfall runoff increases and snowmelt decreases especially in the long term; this can be explained by the fact that more precipitation would fall in the form of rain and less in the form of snow under the warming climate (not shown). For the monsoon-dominated basins UYE, UYA, US, and UM, the increased rainfall runoff is the dominant cause for the total runoff increase. Differently, in the UB, around 60.0–80.0% of the total runoff increase is from the increased glacier-melt water. In the western basin UI, the increased glacier runoff is the dominant cause (80.0–95.0%) for the increased total runoff, which is consistent with the runoff projections for the upper Indus by Lutz et al. (2014).

Fig. 8 presents the contribution of the three runoff components to the total runoff for the study basins under different scenarios. The impact of glacier-melt water on future runoff is minor for the UYE (<1.0% of the total runoff) and moderate for the UM (<4.0% of the total runoff) under all scenarios due to the very limited glacier coverage within these basins (Table 1). However, the impact would become considerable for the US and UYA with about 10.0–12.0% of the total flows from glacier runoff in the long term under RCP8.5. The glacier-melt water would contribute 14.0–21.0% to the total runoff for the UB and 45.0–53.0% for the UI, indicating the critical importance of glacier-melt water on the future runoff in the UB and UI. In response to the increased precipitation and warming climate, all the basins generally show an increase in the contribution of rainfall runoff to the total flows, but a decrease in snowmelt runoff. The contribution of glacier melt to total runoff generally shows an increasing trend for all basins at least until 2070.

For the monsoon-dominated basins UYE, UM, UYA, and US, the future runoff is closely associated with the future precipitation changes although the warming climate enhances evapotranspiration and changes the ratio of solid and liquid precipitation. At the same time, the future runoff changes of the UB and UI are more closely linked to future temperature increases. At the plateau scale, precipitation is mostly projected to increase and the temperature to keep rising for both near term and long term (Figs. 2 and 3). Therefore, due to the increased precipitation

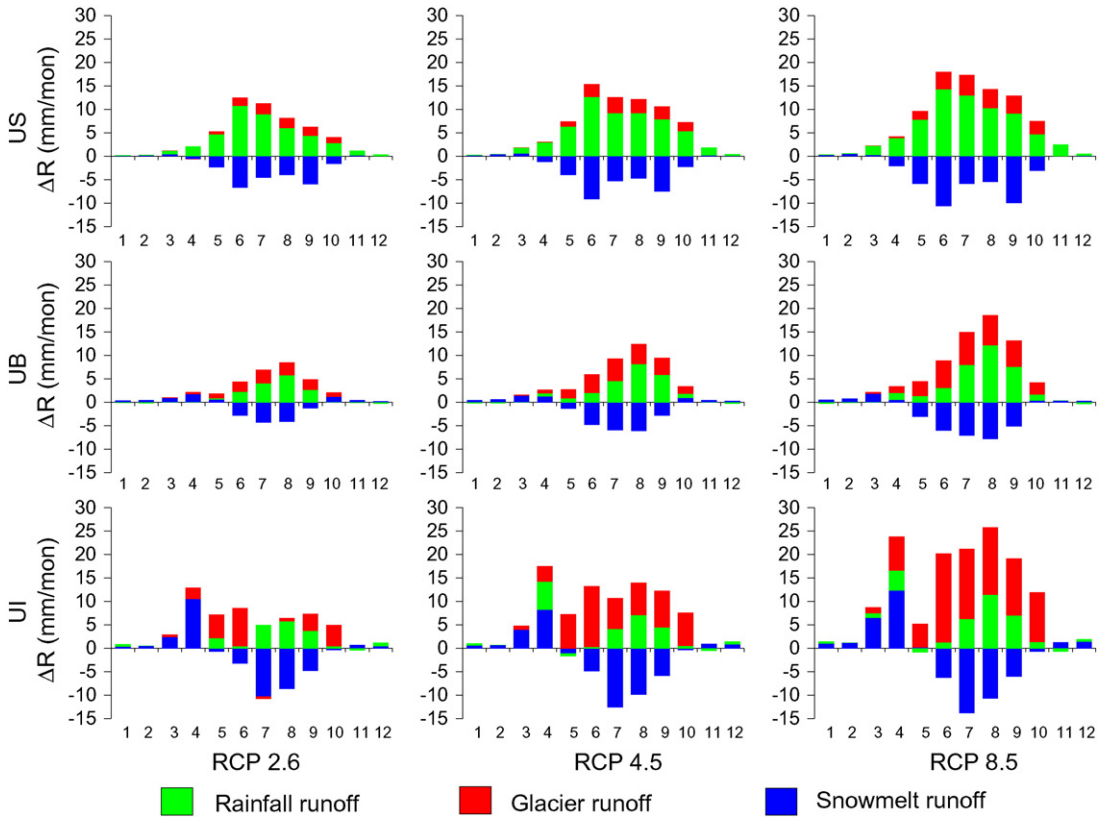

Fig. 11. Seasonal changes of rainfall runoff, snowmelt runoff, and glacier-melt runoff during 2041–2070 relative to the baseline 1971–2000 for the basins US, UB, and UI, under the scenarios considered.

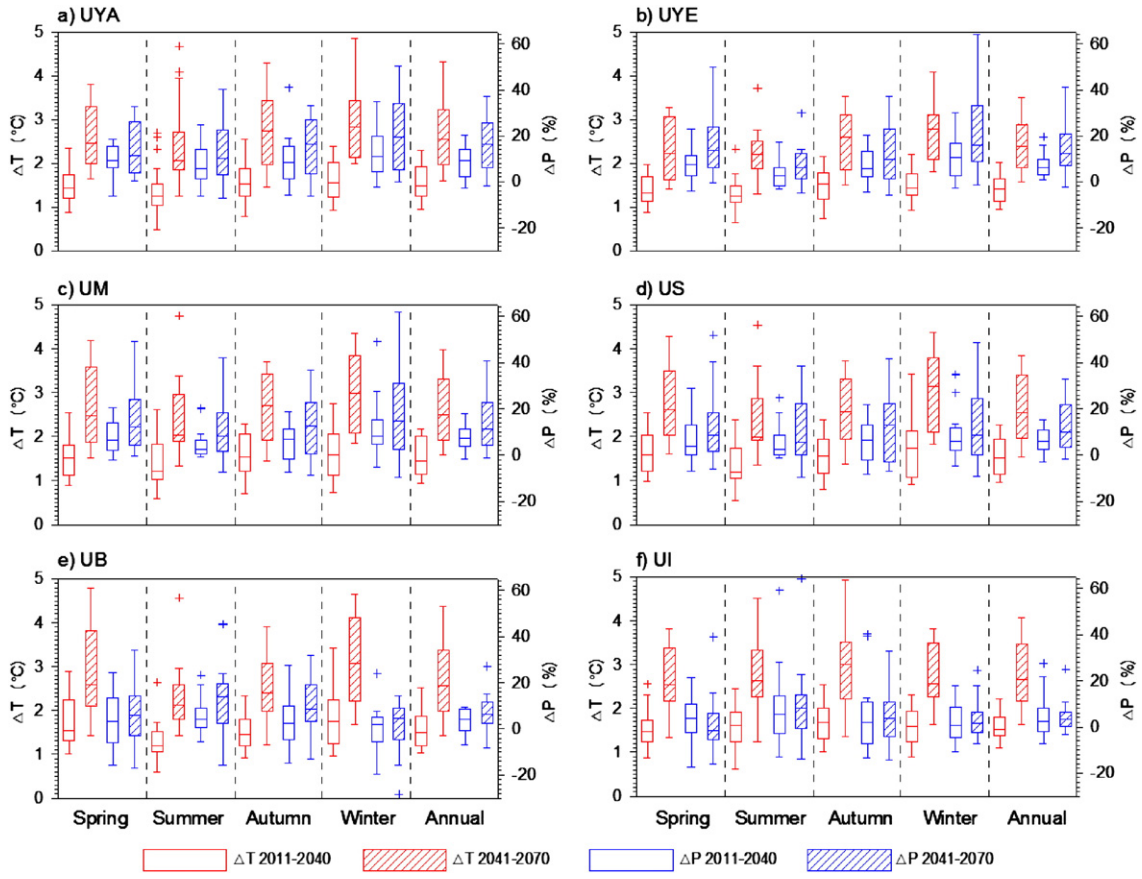

Fig. 12. Projected changes in temperature (°C, indicated by red color) and precipitation (%, indicated by blue color) from the 20 CMIP5 GCMs per basin for 2011–2040 and 2041–2070 with respect to 1971–2000 for scenario RCP4.5. In each pair of box-and-whisker plots, the left one is for 2011–2040 and the right for 2041–2070. Box-and-whisker plots indicate the 10th and 90th percentiles (whiskers), 25th and 75th percentiles (box ends), and median (solid middle bar).

and glacier runoff under the projected warming, we conclude that the total runoff in both the precipitation- and meltwater-dominated basins from the TP is unlikely to decline at least until 2070. This is in line with a recent study (Lutz et al., 2014) that projects an increase in runoff at least until 2050, due primarily to an increase in precipitation in the upper Ganges, Salween and Mekong basins and to accelerated melt in the upper Indus.

4.2. Seasonal changes

The runoff pattern is similar to that for precipitation for the monsoon basins, with 60–80% of annual runoff in June to September, while for the UI, nearly 50% of the annual runoff occurs in July and August mostly resulting from melt water (Zhang et al., 2013). Fig. 9 shows seasonal cycle of simulated runoff for the future. Figs. 10 and 11 presents the seasonal changes of each runoff component. The annual hydrograph remains practically unchanged for all the monsoon-dominated basins (UYE, UYA, UM, US and UB), where large positive rainfall runoff changes generally occur during May–October, during which the snowfall runoff shows negative changes as a result of the warming climate and more precipitation falling in the form of rain. Positive snowmelt runoff is observed in spring months for the UYE, UYA, and UB, indicating an early spring snowmelt over these basins in the long term. For the largely meltwater-dominated UI, glacier runoff has the largest increase among the runoff components during May–October (Fig. 11). We observe an apparent earlier melt and a large increase (51.0–233.0%) in the total runoff for March and April in the long run, which is mostly caused by a dramatic increase in snowmelt runoff, especially in March (Fig. 11). Under the influence of the westerlies, the cold season's precipitation during November to April (mostly in the form of snowfall) accounts for 45.0% of the annual total in the UI, compared to less than 10% in monsoon-dominated basins (Zhang et al., 2013). Melt of winter snowfall and snow cover largely contributes to the spring flows. The large Tarbela dam is highly dependent on the UI inflow and the early melt in spring would increase water availability in the Indus Basin irrigation scheme during the spring growing seasons.

5. Uncertainties in runoff projections

Previous researches (Phillips and Gleckler, 2006; Mote and Salathe, 2010; Su et al., 2013) suggest that multi-model ensemble means generally show better agreement with observations than any single model. In this work, the monthly change factors of precipitation and temperature are based on the means of the 20 GCMs outputs. To illustrate the variety in the GCMs projections, Fig. 12 presents seasonal and mean annual changes in temperature and precipitation from the 20 GCMs for the near term and long term relative to the reference period 1971–2000 for scenario RCP4.5. All the basins exhibit large intermodel variability in both temperature and precipitation, with a larger spread occurring in the long term (1.4–24.8% for precipitation, 1.9–3.4 °C for temperature in annual means for the 25th and 75th percentiles range). This spread is even larger for some seasons (e.g., cold seasons for temperature). To investigate how the spread in climate inputs affects runoff simulations, we chose two representative basins-the UI with the largest glacier coverage, and the UYE with the least impact from the glacier. Fig. 13 shows the mean monthly runoff projections from 20 ensemble members

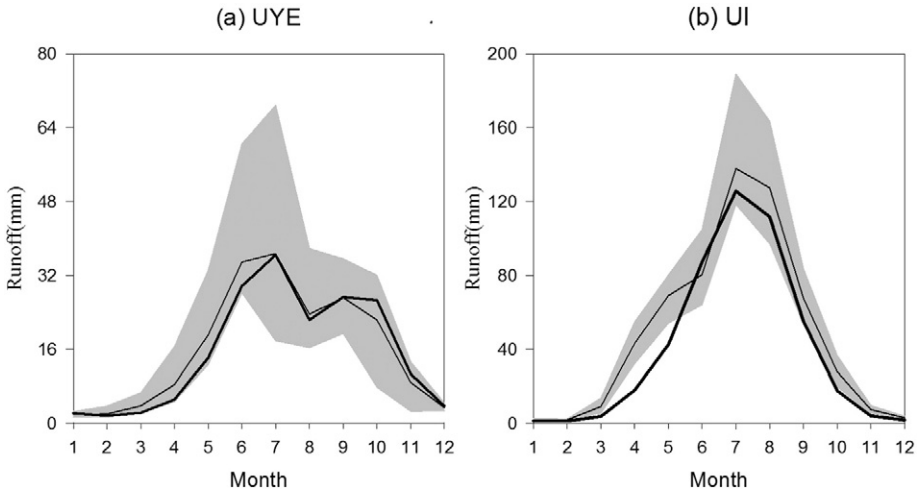

Fig. 13. Mean monthly runoff projections from 20 ensembles scenarios for the monsoon basin UYE (a) and the westerly-dominated basin UI (b) for the 2041–2070 period under RCP4.5. The thin solid line represents the ensemble means, the thick solid line the historic simulations for 1971–2000, and the gray swath represents the spans of results from the 20 ensembles.

for the monsoon basin UYE and the westerly-dominated basin UI for the long term under RCP4.5. We summarize the ensemble projections through use of a gray swath which spans the range of results from the 20 ensemble members.

For the basin UI (Fig. 13b), which is largely temperature-affected, the spread among the GCMs is mostly within 50% of the ensemble mean for each season. Larger discrepancy among the GCMs can be observed in the precipitation dominated basin UYE (Fig. 13a), with the spread mostly more than 100% of the ensemble means. It is noticed that some individual models (MIROC5 for the UI, and GFDL-CM3 for the UYE) stand out which enlarged the spans in the projected runoff. If the two single models are not accounted, the spans among the runoff projections are mostly less than 20% of the ensemble means for the UI, and 50–70% for the UYE for all the seasons. Results in Fig. 13 also suggest that the monsoon basins may have larger uncertainties in runoff projections than the melt-dominated basins (such as the UI), since GCMs tend to have larger uncertainties in precipitation projections than in temperature. Despite the large spread among the runoff projections, the ensemble means general show increase in future runoff relative to the reference period 1971–2000.

The uncertainties in runoff simulations associated with the hydrologic model parameters have been discussed in detail in Zhang et al. (2013). Their results reveal that model uncertainties associated with temperature lapse rate are generally within 3%, while the degree-day factor for ice melt can cause 5% increase in glacier runoff for every 1 unit (mm $°C^{-1}$ day^{-1}) increase. The sensitivity analysis suggests that the changes of model relative errors (Er) are within 4% when b_inf varies from 0 to 0.4, while the bias is more sensitive to d2, with Er reaching −50% when d2 increases to 3.0 m (Zhang et al., 2013). Since the VIC-glacier model has been calibrated and validated with long term observation-based forcing data and streamflow data, the uncertainties in the runoff projections stemming from the climate change projections are much larger than those from the hydrological model itself.

6. Conclusions

In this work, we have assessed the hydrological impacts for the headwater basin of six major rivers in either monsoon- or westerlies-dominated regions in the TP using the well-established VIC-glacier land surface hydrological model driven by composite projections of 20 CMIP5 GCMs under scenarios RCP2.6, RCP4.5, and RCP8.5. The results are summarized as the following:

1. At the plateau scale, annual precipitation is generally projected to increase by 5.0–10.0% in the near term (2011–2040) and 10.0–20.0% in the long term (2041–2070) relative to the reference period 1971–2000, with an increasing south–north gradient. Annual temperature is projected to increase for all scenarios with the greatest warming in the northwest (2.0–4.0 °C) and least in the southeast (1.2–2.8 °C), with the largest warming occurring in the long term.
2. The total runoff of the study basins would either remain stable or moderately increase in the near term, and increase by 2.7–22.4% in the long term relative to the 1971–2000. The increased rainfall runoff is the dominant cause for the total runoff increase for the monsoon-dominated basins UYE, UYA, US, and UM. In the UB, more than 50.0% of the total runoff increase is from the increased glacier-melt water in the long run. Differently, in the western basin UI, the increased glacier runoff is the main cause for the increased total runoff.
3. The glacier-melt water exerts minor impacts on the future runoff of the UYE and moderate effect for the UM due to the limited glacier coverage within these basins. The impact would be considerable for the US and UYA in the long term under RCP8.5 (contributing about 10.0–12.0% of the total flows). The glacier-melt water would be critically important to the future runoff in the UB and UI (contributing about 14.0–21.0% of the total runoff for the UB, and 45.0–53.0% for the UI).
4. The annual hydrograph remains practically unchanged for all the monsoon-dominated basins (UYE, UYA, UM, US and UB). However, for the westerly-controlled basin UI, we observe an apparent earlier melt and a large increase in spring runoff, which may increase water availability in the Indus Basin irrigation scheme during the spring growing seasons.

Acknowledgements

This work was financially supported by the National Natural Science Foundation of China (41190081, 41171051), the “Strategic Priority Research Program (B)” of the CAS (XDB03000000). Deliang Chen is supported by the Swedish Research Council (VR).

References

Adam, J.C., Hamlet, A.F., Lettenmaier, D.P., 2009. Implications of global climate change for snowmelt hydrology in the 21st century. Hydrol. Process. 23 (7), 962–972.
Arendt, A., Bolch, T., Cogley, J.G., Gardner, A., Hagen, J.O., 2012. Randolph Glacier Inventory [v2.0]: a dataset of global glacier outlines. Global Land Ice Measurements from Space, Digital Media, Boulder Colorado, USA.

Bahr, D.B., Meier, M.F., Peckham, S.D., 1997. The physical basis of glacier volume–area scaling. J. Geophys. Res. 102 (B9), 20355–20362.

Barnett, T.P., Adam, J.C., Lettenmaier, D.P., 2005. Potential impacts of a warming climate on water availability in snow-dominated regions. Nature 438, 303–309.

Beyene, T., Lettenmaier, D.P., Kabat, P., 2010. Hydrologic impacts of climate change on the Nile River Basin: implications of the 2007 IPCC scenarios. Clim. Chang. 100, 433–461.

Bliss, A., Hock, R., Radić, V., 2014. Global response of glacier runoff to twenty-first century climate change. J. Geophys. Res. 119, 1–14.

Bolch, T., Kulkarni, A., Kääb, A., Huggel, C., Paul, F., Cogley, J.G., Frey, H., Kargel, J.S., Fujita, K., Scheel, M., Bajracharya, S., Stoffel, M., 2012. The state and fate of himalayan glaciers. Science 336, 310–314.

Bookhagen, B., Burbank, D.W., 2010. Toward a complete Himalayan hydrological budget: spatiotemporal distribution of snowmelt and rainfalland their impact on river discharge. J. Geophys. Res. 115, F03019. http://dx.doi.org/10.1029/2009JF001426.

Cherkauer, K.A., Lettenmaier, D.P., 1999. Hydrologic effects of frozen soils in the upper Mississippi River basin. J. Geophys. Res. 104 (D16), 19599–19610.

Cherkauer, K.A., Lettenmaier, D.P., 2003. Simulation of spatial variability in snow and frozen soil. J. Geophys. Res. 108 (D22), 8858. http://dx.doi.org/10.1029/2003JD003575.

Christensen, N., Lettenmaier, D.P., 2007. A multimodel ensemble approach to assessment of climate change impacts on the hydrology and water resources of the Colorado River basin. Hydrol. Earth Syst. Sci. 11, 1417–1434.

Christensen, N.S., Wood, A.W., Voisin, N., Lettenmaier, D.P., Palmer, R.N., 2004. The effects of climate change on the hydrology and water resources of the Colorado River basin. Clim. Chang. 62, 337–363.

Cubasch, U., Wuebbles, D., Chen, D., Facchini, M.C., Frame, D., Mahowald, N., Winter, J.-G., 2013. Introduction. In: Stocker, T.F., Qin, D., Plattner, G.-K., Tignor, M., Allen, S.K., Boschung, J., Nauels, A., Xia, Y., Bex, V., Midgley, P.M. (Eds.), Climate Change 2013: The Physical Science Basis. Contribution of Working Group I to the Fifth Assessment Report of the Intergovernmental Panel on Climate Change. Cambridge University Press, Cambridge, United Kingdom and New York, NY, USA (1535 pp.).

Cuo, L., Beyene, T.K., Voisin, N., Su, F., Lettenmaier, D.P., Alberti, M., Richey, J.E., 2011. Mid-21st century climate and land cover change effects on the hydrology of the Puget Sound basin, Washington. Hydrol. Process. 25 (11), 1729–1753.

Elsner, M.M., Cuo, L., Voisin, N., Deems, J.S., Hamlet, A.F., Vano, J.A., Mickelson, K.E.B., Lee, S.Y., Lettenmaier, D.P., 2010. Implications of 21st Century climate change for the hydrology of Washington State. Clim. Chang. 102, 225–260.

Frauenfeld, O.W., Zhang, T., Serreze, M.C., 2005. Climate change and variability using European Centre for Medium-Range Weather Forecasts reanalysis (ERA-40) temperatures on the Tibetan Plateau. J. Geophys. Res. 110, D02101. http://dx.doi.org/10.1029/2004JD005230.

Gleick, P.H., 1986. Methods for evaluating the regional hydrologic effects of global climate changes. J. Hydrol. 88, 97–116.

Hamlet, A.F., Lettenmaier, D.P., 1999. Effects of climate change on hydrology and water resources of the Columbia River basin. J. Am. Water Resour. Assoc. 35 (6), 1597–1624.

Hay, L.E., Wilby, R., Leavesley, G.H., 2000. A comparison of delta change and downscaled GCM scenarios for three mountainous basins in the United States. J. Am. Water Resour. Assoc. 36 (2), 387–397.

Hayhoe, K., Wake, C., Huntington, T.G., Luo, L., Schwartz, M.D., Sheffield, J., Wood, E.F., Anderson, B., Bradbury, J., DeGaetano, T.T., Wolfe, D., 2007. Past and future changes in climate and hydrological indicators in the US Northeast. Clim. Dyn. 28, 381–407.

Hock, R., 2003. Temperature index melt modelling in mountain areas. J. Hydrol. 282, 104–115.

Immerzeel, W.W., Droogers, P., De Jong, S.M., Bierkens, M.F., 2009. Large-scale monitoring of snow cover and runoff simulation in Himalayan river basins using remote sensing. Remote Sens. Environ. 113, 40–49.

Immerzeel, W.W., Pellicciotti, F., Bierkens, M.F.P., 2013. Rising river flows throughout the twenty-first century in two Himalayan glacierized watersheds. Nat. Geosci. 6, 742–745.

Immerzeel, W.W., van Beek, L.P.H., Bierkens, M.F., 2010. Climate change will affect the Asian water towers. Science 328, 1382–1385.

Immerzeel, W.W., van Beek, L.P.H., Konz, M., Shrestha, A.B., Bierkens, M.F.P., 2012. Hydrological response to climate change in a glacierized catchment in the Himalayas. Clim. Chang. 110, 721–736.

Jeelani, G., Feddema, J.J., van der Veen, C.J., Stearns, L., 2012. Role of snow and glacier melt in controlling river hydrology in Liddar watershed (western Himalaya) under current and future climate. Water Resour. Res. 48, W12508.

Kaser, G., Großhauser, M., Marzeion, B., 2010. Contribution potential of glaciers to water availability in different climate regimes. Proc. Natl. Acad. Sci. U. S. A. 107 (47), 20223–20227.

Liang, X., Lettenmaier, D.P., Wood, E.F., Burges, S.J., 1994. A simple hydrologically based model of land surface water and energy fluxes for general circulation models. J. Geophys. Res. 99 (D17), 14415–14428.

Liang, X., Wood, E.F., Lettenmaier, D.P., 1996. Surface soil moisture parameterization of the VIC-2 L model: evaluation and modification. Glob. Planet. Chang. 13, 195–206.

Liu, X., Chen, B., 2000. Climatic warming in the Tibetan Plateau during recent decades. Int. J. Climatol. 20, 1729–1742.

Liu, S., Sun, W., Shen, Y., Li, G., 2003. Glacier changes since the Little Ice Age maximum in the western Qilian Shan, northwest China, and consequences of glacier runoff for water supply. J. Glaciol. 49, 117–124.

Lohmann, D., Raschke, E., Nijssen, B., Lettenmaier, D.P., 1998. Regional scale hydrology: I. Formulation of the VIC-2 L model coupled to a routing model. Hydrol. Sci. J. 43, 131–141.

Lutz, A.F., Immerzeel, W.W., Shrestha, A.B., Bierkens, M.F.P., 2014. Consistent increase in high Asia's runoff due to increasing glacier melt and precipitation. Nat. Clim. Chang. 4, 87–592.

Maurer, E.P., 2007. Uncertainty in hydrologic impacts of climate change in the Sierra Nevada California under two emissions scenarios. Clim. Chang. 82, 309–325.

Maurer, E.P., Wood, A.W., Adam, J.C., Lettenmaier, D.P., Nijssen, B., 2002. A long-term hydrologically based dataset of land surface fluxes and states for the conterminous United States. J. Clim. 15, 3237–3251.

Moss, R.H., et al., 2010. The next generation of scenarios for climate change research and assessment. Nature 463, 747–756.

Mote, P.W., Salathe, E.P., 2010. Future climate in the Pacific Northwest. Clim. Chang. 109, 29–50.

Nijssen, B.N., O'Donnell, G.M., Lettenmaier, D.P., Wood, E.F., 2001. Predicting the discharge of global rivers. J. Clim. 14, 3307–3323.

Payne, J.T., Wood, A.W., Hamlet, A.F., Palmer, R.N., Lettenmaier, D.P., 2004. Mitigating the effects of climate change on the water resources of the Columbia River basin. Clim. Chang. 62, 233–256.

Phillips, T.J., Gleckler, P.J., 2006. Evaluation of continental precipitation in 20th century climate simulations: the utility of multimodel statistics. Water Resour. Res. 42, W03202.

Radić, V., Hock, R., 2010. Regional and global volumes of glaciers derived from statistical upscaling of glacier inventory data. J. Geophys. Res. 115, F01010. http://dx.doi.org/10.1029/2009JF001373.

Radić, V., Hock, R., Oerlemans, J., 2007. Volume–area scaling vs flowline modelling in glacier volume projections. Ann. Glaciol. 46, 234–240.

Radić, V., Hock, R., Oerlemans, J., 2008. Analysis of scaling methods in deriving future volume evolutions of valley glaciers. J. Glaciol. 54, 601–612.

Rees, H.G., Collins, D.N., 2006. Regional differences in response of flow in glacier-fed Himalayan rivers to climatic warming. Hydrol. Process. 20, 2157–2169.

Singh, P., Bengtsson, L., 2005. Impact of warmer climate on melt and evaporation for the rainfed, snowfed and glacierfed basins in the Himalayan region. J. Hydrol. 300, 140–154.

Storck, P., Lettenmaier, D.P., 1999. Predicting the effect of a forest canopy on ground snow accumulation and ablation in maritime climates. 67th Western Snow Conference, edited by C. Troendle. Colo. State Univ., pp. 1–12.

Su, F., Adam, J.C., Bowling, L.C., Lettenmaier, D.P., 2005. Streamflow simulations of the terrestrial Arctic domain. J. Geophys. Res. 110, D08112. http://dx.doi.org/10.1029/2004JD005518.

Su, F., Duan, X., Chen, D., Hao, Z., Cuo, L., 2013. Evaluation of the Global Climate Models in the CMIP5 over the Tibetan Plateau. J. Clim. 26, 3187–3208.

Tahir, A.A., Chevallier, P., Arnaud, Y., Neppel, L., Ahmad, B., 2011. Modeling snowmelt-runoff under climate scenarios in the Hunza River basin, Karakoram Range, Northern Pakistan. J. Hydrol. 409, 104–117.

Taylor, K.E., Stouffer, R.J., Meehl, G.A., 2012. An overview of CMIP5 and the experiment design. Bull. Am. Meteorol. Soc. 93, 485–498.

Thompson, L.G., Yao, T., Mosley-Thompson, E., Davis, M.E., Henderson, K.A., Lin, P.N., 2000. A high-resolution millennial record of the South Asian monsoon from Himalayan ice cores. Science 289, 1916–1919.

Tong, K., Su, F., Yang, D., Zhang, L., Hao, Z., 2014. Tibetan Plateau precipitation as depicted by gauge observations, reanalyses and satellite retrievals. Int. J. Climatol. 34, 265–285.

Vicuna, S., Maurer, E.P., Joyce, B., Dracup, J.A., Purkey, D., 2007. The sensitivity of California water resources to climate change scenarios. J. Am. Water Resour. Assoc. 43, 482–498.

van Vuuren, D.P., Edmonds, J., Kainuma, M., Riahi, K., Thomson, A., Hibbard, K., Hurtt, G.C., Kram, T., Krey, V., Lamarque, J., Masui, T., Meinshausen, M., Nakicenovic, N., Smith, J., Rose, S.K., 2011. The representative concentration pathways: an overview. Clim. Chang. 109, 5–31.

Wang, B., Bao, Q., Hoskins, B., Wu, G., Liu, Y., 2008. Tibetan Plateau warming and precipitation changes in East Asia. Geophys. Res. Lett. 35, L14702. http://dx.doi.org/10.1029/2008GL034330.

Wu, S., Yin, Y., Zheng, D., Yang, Q., 2007. Climatic trends over the Tibetan Plateau during 1971–2000. J. Geogr. Sci. 17, 141–151.

Xu, Z., Gong, T., Li, J., 2008. Decadal trend of climate in the Tibetan Plateau-regional temperature and precipitation. Hydrol. Process. 22, 3056–3065.

Yao, T., Liu, X., Wang, N., Shi, Y., 2000. Amplitude of climatic changes in Qinghai-Tibetan Plateau. Chin. Sci. Bull. 45, 1236–1243.

Yao, T., Pu, J., Lu, A., Wang, Y., Yu, W., 2007. Recent glacial retreat and its impact on hydrological processes on the Tibetan Plateau, China, and surrounding regions. Arct. Antarct. Alp. Res. 39, 642–650.

Yao, T., Ren, J., Xu, B., 2008. Map of Glaciers and Lakes on the Tibetan Plateau and the Surroundings. Xi'an Cartographic Publishing House.

Yao, T., Thompson, L., Yang, W., Yu, W., Gao, J., Guo, X., Yang, X., Duan, K., Zhao, H., Xu, B., Pu, J., Lu, A., Xiang, Y., Kattel, D.B., Joswiak, D., 2012. Different glacier status with atmospheric circulations in Tibetan Plateau and surroundings. Nat. Clim. Chang. 2, 663–667.

Yao, T., Wang, Y., Liu, S., Pu, J., Shen, Y., Lu, A., 2004. Recent glacial retreat in High Asia in China and its impact on water resource in Northwest China. Sci. China. Ser. D 47 (12), 1065–1075.

Yatagai, A., Arakawa, O., Kamiguchi, K., Kawamoto, H., Nodzu, M.I., Hamada, A., 2009. A 44-year daily gridded precipitation dataset for Asia based on a dense network of rain gauges. SOLA 5, 137–140.

Zhang, L., Su, F., Yang, D., Hao, Z., Tong, K., 2013. Discharge regime and simulation for the upstream of major rivers over Tibetan Plateau. J. Geophys. Res. 118. http://dx.doi.org/10.1002/jgrd.50665.